Int. J. Electrochem. Sci., 8 **(2013)** 9435 - 9441

International Journal of
ELECTROCHEMICAL
SCIENCE
www.electrochemsci.org

Short Communication

Hydrogen Production from Rapid Auto-decomposition of Formic Acid at Room Temperature on Electrodeposited Foam Films of Nanodendritic AuPd and AgPd

Jun Liu, Ling Cao, Yue Xia, Wei Huang, Zelin Li[*]

Key Laboratory of Chemical Biology and Traditional Chinese Medicine Research (Ministry of Education of China), College of Chemistry and Chemical Engineering, Hunan Normal University, Changsha 410081, China
[*]E-mail: lizelin@hunnu.edu.cn

Received: 8 May 2013 / *Accepted:* 11 June 2013 / *Published:* 1 July 2013

In this communication, we report an unusual observation on vigorous gas release of H_2 and CO_2 from rapid auto-decomposition of formic acid at room temperature on nanodendritic AuPd and AgPd foam films. These new binary noble metal foams were prepared by electrodeposition under strongly cathodic polarization. The high catalytic activity was contributed to the abundant active sites such as steps, corners, kinks, edges and atomic dislocations in the nanodendrites comprised of nanoparticles, as well as to the electronic effect of binary metals.

Keywords: Nanodendrites, binary noble metal foams, electrodeposition, hydrogen production, auto-decomposition of formic acid

1. INTRODUCTION

Since the pioneer work of Liu and his co-workers on electrodeposition of common metal foam films of Cu and Sn utilizing hydrogen bubble dynamic templates [1], this convenient electrodeposition technique under strongly cathodic polarization has recently been extended to fabricate some single and binary noble metal foam films such as Ag [2], Au [3-4], Pt [5], Pd [6], AuPt [7], and PdPt [8]. These foam films demonstrated strong surface enhanced Raman scattering (SERS) [4] and high electrocatalytic activity towards oxidation of small organic molecules [4-8]. Optimistically, new binary noble foam films with unusual properties are still expected and need further exploration.

In this work, we prepared new binary noble metal foam films of AuPd and AgPd comprised of nanodendritic walls by direct electrodeposition on Au and Ti substrates under strongly cathodic

polarization, and observed an unusual phenomenon that these foam films can automatically decompose formic acid at room temperature to produce high-quality hydrogen gas very rapidly. These supported foam films are expected to become a new category of promising nanocatalysts for hydrogen production from auto-decomposition of formic acid at room temperature, apart from dispersed nanoparticles [9-11] and homogeneous catalysts [12-14].

2. EXPERIMENTALPART

2.1. Reagents and materials

$HAuCl_4 \cdot 4H_2O$, $AgNO_3$, $Pd(C_2H_3O_2)_2$, $PdCl_2$, H_2SO_4, HCOOH and HCOONa were all of analytical grade. All solutions were freshly prepared using Milli-Q water (Millipore).

2.2. Electrodeposition of foam films

Electrodeposition of AuPd foam films onto a gold disk (1 mm diameter) were performed on a 660C electrochemical workstation (Chenhua, China) with a three-electrode configuration under a constant potential of –4 V vs. saturated mercurous sulfate electrode (SMSE) for 300 s in a solution of 2 mM $HAuCl_4$ + 0.58 mM $PdCl_2$ + 2 M H_2SO_4, 1 mM $HAuCl_4$ + 1 mM $PdCl_2$ + 2 M H_2SO_4, or 0.5 mM $HAuCl_4$ + 1.5 mM $PdCl_2$ + 2 M H_2SO_4. We denoted the deposited foam films as $Au_{100}Pd_{29}$, Au_1Pd_1, and Au_1Pd_3, respectively, according to the mole ratio of $HAuCl_4/PdCl_2$ in the feeding solution. Ag_1Pd_1 foam films were also prepared by electrodeposition under −4 V for 300 s with a precursor solution of 1 mM $AgNO_3$ + 1 mM $Pd(C_2H_3O_2)_2$ + 2 M H_2SO_4.

We also electrodeposited the foam films onto a larger Ti plate (geometric area 2 cm^2) substrate under a constant voltage of −7 V for 200 s with a direct current (DC) power (KXN-1550D) and a two-electrode configuration, where a large platinum foil was employed as the counter electrode. Prior to use, the Ti plates were polished with 2000 grit carbimet paper, etched in 18% HCl at 85 °C for 15 min, and washed with Milli-Q water.

2.3 Determination of real surface areas

The real surface areas of the prepared foam films were estimated from the double layer capacity measurement and the details of experiments and calculation were described in Ref. [15].

2.4. Characterization

Morphologies of the foam films were taken with a JEOL JSM-6360 scanning electron microscope (SEM) and a JEOL-1230 transmission electron microscope (TEM). Their bulk compositions were analyzed with an energy-dispersive X-ray (EDX) spectrometer. X-ray diffraction (XRD) patterns were obtained with a Dmax Rapid IIR diffractometer using Cu K□ (0.1542 nm) radiation.

2.5. Catalytic decomposition of formic acid and product analysis

Catalytic decomposition of formic acid by the deposited foam films was performed at room temperature (~25 ^{o}C) either in a test tube or in a beaker containing a solution of 6.64 M HCOOH and 3.32 M HCOONa. For analysis of gas chromatography (GC 5890F) [16] the produced gases were collected by the draining water method using a glass funnel and a gas-collecting bottle (35 mL) that were placed upside down. In addition, a graduated gas-collecting tube was used to record the gas volume released during 2 h.

The deposited foam catalysts can be used repeatedly after being washed with Milli-Q water and dried under an infrared lamp, or treated by potential cycling in 1 M H_2SO_4 within the potential range of –0.65 to 1 V at a scan rate of 100 mV s^{-1}.

3. RESULTS AND DISCUSSION

3.1. Characterizations of the electrodeposited foam films

The SEM images in Fig. 1(a-d) show the porous structures of the prepared AuPd and Ag_1Pd_1 foam films by electrodeposition on Au disk electrodes (1 mm diameter). The hierarchical pores in the foams were highly interconnected, and the walls were comprised of nanodendrites (the inset), of which in AgPd foams were smaller and thinner.

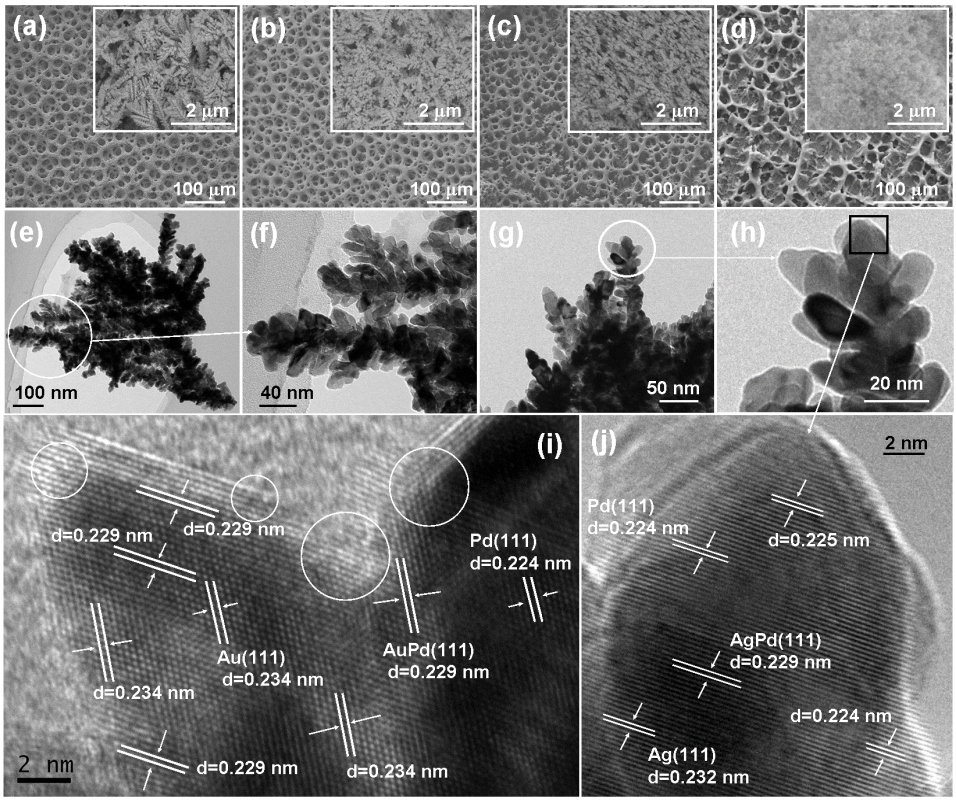

Figure 1. SEM images of electrodeposited foam films of (a) $Au_{100}Pd_{29}$, (b) Au_1Pd_1, (c) Au_1Pd_3 and (d) Ag_1Pd_1, and their TEM and HR-TEM images of (e, f, i) Au_1Pd_1, and (g, h, j) Ag_1Pd_1.

The detailed dendritic structures of Au_1Pd_1 and Ag_1Pd_1 foams were further demonstrated by TEM and high-resolution TEM (HR-TEM). It can be seen from TEM images of Fig. 1(e-f) and Fig. 1(g-h) that the Au_1Pd_1 and Ag_1Pd_1 dendrites were formed by assembly of nanocrystals sizing from 10-30 nm and 10-20 nm, respectively. The HR-TEM image in Fig. 1(i) reveals the atom lattices of Au_1Pd_1 nanodendrites. The lattice fringe spacings of 0.234 nm, 0.224 nm and 0.229 nm correspond to the interplanar distance of Au(111), Pd(111) and AuPd(111) planes, respectively. Some Au(111) and Pd(111) planes were retained as the Au_1Pd_1 foam film was electrodeposited rapidly under intense polarization, resulting in mixed patterns in the nanoalloy [17]. Such a nanodendritic structure contained abundant active sites such as steps, corners, kinks, edges, and atomic dislocations (indicated with cycles in Fig. 1(i)), which are beneficial for catalysis. Similar situation was also observed in Fig. 1(j) in the HR-TEM image of an AgPd nanodendritic sprout. The lattice fringe spacings of 0.224/0.225 nm, 0.232 nm and 0.229 nm correspond to the interplanar distance of Pd(111), Ag(111) and AgPd(111) planes, respectively.

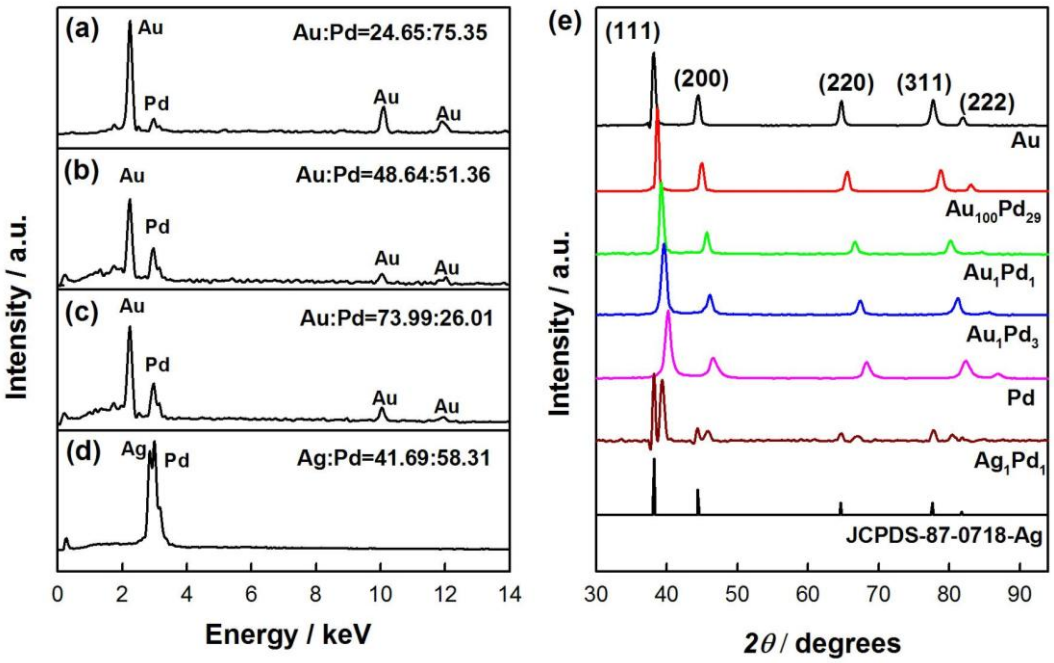

Figure 2. EDX spectra for the foam films of (a) $Au_{100}Pd_{29}$, (b) Au_1Pd_1, (d) Au_1Pd_3 and (d) Ag_1Pd_1. (e) XRD patterns for the foam films of Au, Pd, AuPd and Ag_1Pd_1.

The EDX spectra in Fig. 2(a-d) confirmed that the atomic compositions of AuPd foams were roughly consistent with those of their corresponding precursor solutions. However, the atomic percentage of Pd in the AgPd foam was somewhat higher than that in the solution, which would be due to displacement reaction between deposited Ag and Pd^{2+} in solution.

XRD patterns of the deposited foam films of Pd, Au, AuPd and AgPd as well as the standard card of cubic Ag (JCPDS 87-0718) were shown in Fig. 2e. The diffraction peaks of $Au_{100}Pd_{29}$, Au_1Pd_1, and Au_1Pd_3 samples fall well between those of pure Au and Pd, revealing that the bulk phase of AuPd foams was alloy. For the Ag_1Pd_1 foam, the diffraction peaks of (111), (200), (220) and (311) planes both from pure Ag and from AgPd alloy appeared, suggesting that the AgPd foam film was a mixture

of metallic Ag and AgPd alloy.

3.2. Hydrogen production from formic acid decomposition on the prepared foam films

We found that the foam films of Au, Pd, AuPd and AgPd alloys deposited on Au disk electrodes exhibited high catalytic activity in hydrogen generation from decomposition of formic acid at room temperature (~ 25 °C). As demonstrated in Fig. 3(a), vigorous gas release occurred as soon as the foam film electrodes were immersed in the solution of 6.64 M HCOOH + 3.32 M HCOONa, especially for the Au_1Pd_1 and Ag_1Pd_1 foam films. These unusual phenomena would be largely due to the special nanodendritic structures of the deposited foams (Fig. 1), which had abundant active sites as we mentioned above.

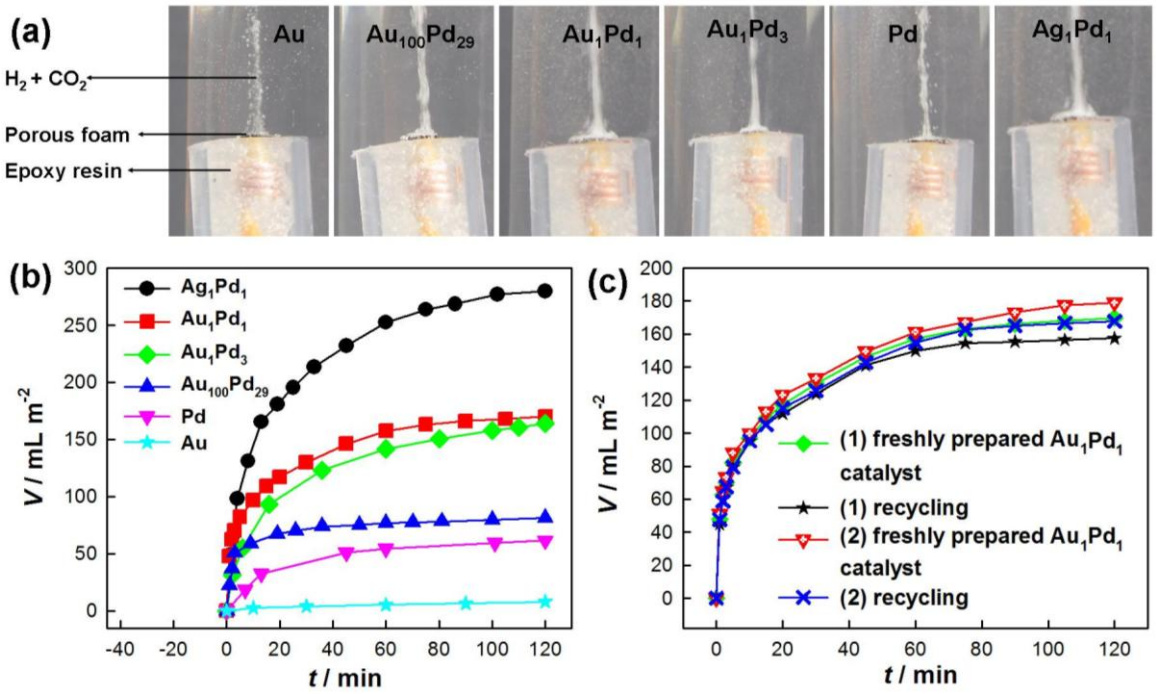

Figure 3. (a) Photos for the hydrogen production at room temperature from the decomposition of formic acid on the foam films deposited on gold disk electrodes (1 mm diameter). The solution in test tubes was 6.64 M HCOOH + 3.32 M HCOONa. (b) The output volume of reforming gas (H_2 + CO_2) during 120 min on the foam films of Au, $Au_{100}Pd_{29}$, Au_1Pd_1, Au_1Pd_3, Pd, and Ag_1Pd_1. (c) Cycling performances of the Au_1Pd_1 foam film renewed by (1) drying in air or (2) by cyclic voltammetry in 1 M H_2SO_4 solution.

To produce more gas from formic acid decomposition we used the larger Ti plate (geometric area 2 cm^2) as substrate to deposit these foam films. Fig. 3(b) shows the relationship between collected volume (based on unit active area) of reforming gas (H_2 + CO_2) and collection time during 2 h with various foam films of Au, $Au_{100}Pd_{29}$, Au_1Pd_1, Au_1Pd_3, Ag_1Pd_1 and Pd in 6.64 M HCOOH and 3.32 M HCOONa solution. Apparently, pure Au and Pd foam films had a lower activity than that of AuPd and AgPd foam films, which can be attributed to the electronic effect between binary metals [18-19].

Among the three AuPd foam films, Au_1Pd_1 showed the highest catalytic activity, which gave a maximum output of 169.8 mL m^{-2} reforming gas in 2 h. Especially, the original reaction rate was extremely fast and about 48.09 mL m^{-2} reforming gas was released in the first 1 min, being 28.31% of the total reforming gas in 120 min. The reaction rate then became steady after 20 min. The CO content in the reforming gas from the minor reaction of $HCOOH = CO + H_2O$ was determined to be 65 ppm by gas chromatography. So, the decomposition of formic acid mainly proceeded via the reaction of $HCOOH = H_2 + CO_2$. Moreover, the content of CO_2 was detected to be 8.15% (less than 50%) because of dissolution in solution in view of the large volume of the HCOOH + HCOONa solution (2 L) we used to collect the gases conveniently. The turnover frequency (TOF) [10] of the main reaction during 2 h on the Au_1Pd_1 alloy foam was up to 188 h^{-1} at room temperature (25 °C), better than most literatures [20]. Ag_1Pd_1 foam film was the best catalyst among the six foam films, which gave a maximum output of 279.5 mL m^{-2} reforming gas in 2 h.

The catalytic activity of the foam film can be easily renewed by cleaning them in pure water and followed by drying in air under an infrared lamp for 2 h or by cyclic voltammetry in H_2SO_4 solution. The released gas volumes were almost the same for the repeated performances, especially in the first 20 min (Fig. 3c).

4. CONCLUSIONS

In summary, we have prepared new binary noble metal foam films of AuPd and AgPd by electrodeposition under highly cathodic polarization. We found that the foam films of Au_1Pd_1 and Ag_1Pd_1 could rapidly decompose formic acid into hydrogen gas as well as carbon dioxide at room temperature (~ 25 °C). The high catalytic activity of the foam films is attributed to the abundant active sites on the nanodendrites and the electronic effect of binary metals. Such supported thin films of nanocatalysts are convenient for controlling, separating and recycling in comparison with dispersed nanoparticles and homogeneous catalysts reported in literature. Although improvements are still required to further enhance the catalytic activity and selectivity, our findings here may open a new avenue to develop supported solid film nanocatalysts for hydrogen production from auto-decomposition of formic acid in aqueous solution.

ACKNOWLEDGEMENTS

We appreciate financial supports from NNSF of China (Grant Nos. 21173075 and 21003045), and Ph. D. Programs Foundation of the Education Ministry of China (Grant No. 20104306110003).

References

1. H. C. Shin, J. Dong, M. L. Liu, *Adv. Mater.*, 15 (2003) 1610.
2. S. Cherevko, X. L. Xing, H. C. Chung, *Electrochem. Commun.*, 12 (2010) 467.
3. S. Cherevko, C. H. Chung, *Electrochem. Commun.*, 13 (2011) 16.
4. B. J. Plowman, A. P. O'Mullane, P. R. Selvakannan, S. K. Bhargava, *Chem. Commun.*, 46 (2010) 9182.

5. A. Ott, L. A. Jones, S. K. Bhargava, *Electrochem. Commun*., 13 (2011) 1248.
6. S. Cherevko, N. Kulyk, C. H. Chung, *Nanoscale*, 4 (2012) 103.
7. J. Liu, L. Cao, W. Huang, Z. L. Li, *ACS Appl. Mater. Interfaces*, 3 (2011) 3552.
8. J. Liu, L. Cao, W. Huang, Z. L. Li, *J. Electroanal. Chem.*, 686 (2012) 38.
9. Z. L. Wang, J. M. Yan, H. L. Wang, Y. Ping, Q. Jiang, *Sci. Rep*., 2 (2012) 598.
10. K. Tedsree, T. Li, S. Jones, C. W. A. Chan, K. M. K. Yu, P. A. J. Bagot, E. A. Marquis, G. D. W. Smith, S. C. E. Tsang, *Nature Nanotech*., 6 (2011) 302.
11. X. C. Zhou, Y. J. Huang, W. Xing, C. P. Liu, J. H. Liao, T. H. Lu, *Chem. Commun.*, 30 (2008) 3540.
12. B. Loges, A. Boddien, H. Junge, M. Beller, *Angew. Chem. Int. Ed*., 47 (2008) 3962.
13. A. Boddien, D. Mellmann, F. Gärtner, R. Jackstell, H. Junge, P. J. Dyson, G. Laurenczy, R. Ludwig, M. Beller, *Science*, 333 (2011) 1733.
14. A. Boddien, B. Loges, F. Gärtner, C. Torborg, K. Fumino, H. Junge, R. Ludwig, M. Beller, *J. Am. Chem. Soc*., 132 (2010) 8924.
15. M. Łukaszewski, A. Czerwiński, *Thin Solid Films*, 518 (2010) 3680.
16. R. B. King, N. K. Bhattacharyya, K. D. Wiemers, *Environ. Sci. Technol.*, 30 (1996) 1292.
17. R. Ferrando, J. Jellinek, R. L. Johnston, *Chem. Rev*., 108 (2008) 846.
18. A. E. Baber, H. L. Tierney, E. C. H. Sykes, *ACS Nano*, 4 (2010) 1637.
19. D. A. Slanac, W. G. Hardin, K. P. Johnston, K. J. Stevenson, *J. Am. Chem. Soc.*, 134 (2012) 9812.
20. M. Grasemann, G. Laurenczy, *Energy Environ. Sci*., 5 (2012) 8171.